

Dwell Time Analysis of a Single-Molecule Mechanochemical Reaction[†]

Robert Szoszkiewicz,^{*,‡} Sri Rama Koti Ainavarapu,[‡] Arun P. Wiita,[‡] Raul Perez-Jimenez,[‡] Jose M. Sanchez-Ruiz,[§] and Julio M. Fernandez^{*,‡}

Department of Biological Sciences, Columbia University, New York, New York 10027, and Facultad de Ciencias, Departamento de Química Física, Universidad de Granada, 18071 Granada, Spain

Received August 2, 2007. In Final Form: September 17, 2007

Force-clamp spectroscopy is a novel technique for studying mechanochemistry at the single-bond level. Single disulfide bond reduction events are accurately detected as stepwise increases in the length of polyproteins that contain disulfide bonds and that are stretched at a constant force with the cantilever of an atomic force microscope (AFM). The kinetics of this reaction has been measured from single-exponential fits to ensemble averages of the reduction events. However, exponential fits are notoriously ambiguous to use in cases of kinetic data showing multiple reaction pathways. Here we introduce a dwell time analysis technique, of widespread use in the single ion channel field, that we apply to the examination of the kinetics of reduction of disulfide bonds measured from single-molecule force-clamp spectroscopy traces. In this technique, exponentially distributed dwell time data is plotted as a histogram with a logarithmic time scale and a square root ordinate. The advantage of logarithmic histograms is that exponentially distributed dwell times appear as well-defined peaks in the distribution, greatly enhancing our ability to detect multiple kinetic pathways. We apply this technique to examine the distribution of dwell times of 4488 single disulfide bond reduction events measured in the presence of two very different kinds of reducing agents: tris-(2-carboxyethyl)-phosphine hydrochloride (TCEP) and the enzyme thioredoxin (TRX). A different clamping force is used for each reducing agent to obtain distributions of dwell times on a similar time scale. In the case of TCEP, the logarithmic histogram of dwell times showed a single peak, corresponding to a single reaction mechanism. By contrast, similar experiments done with TRX showed two well-separated peaks, marking two distinct modes of chemical reduction operating simultaneously. These experiments demonstrate that dwell time analysis techniques are a powerful approach to studying chemical reactions at the single-molecule level.

Introduction

Mechanochemistry aims to explain the effects of external mechanical force in activating the rupture of chemical bonds.^{1,2} Mechanochemical reactions in the bulk involve the simultaneous failure of many bonds with intervention by the shear forces, internal friction, defects and other complicated processes. Thus, it remains challenging to relate rupture forces determined in bulk materials to the processes occurring on the local scale.

With the advent of experimental techniques that can manipulate single molecules using mechanical,^{3–5} electrical,⁶ chemical,⁷ and hydrodynamic^{8,9} force, the conformational changes in individual molecules and their mechanical properties can be addressed with subnanometer resolution. The rupture kinetics of individual bonds can be monitored one atom at a time, and the number of reaction pathways can be uniquely characterized by the ensemble of the corresponding rate constants.

Disulfide bond reduction in proteins (i.e., the reversible cleavage of a covalent bond formed between thiol (–SH) groups

of cysteine residues in the presence of reducing agents) is an important aspect of biomechanochemistry.^{10,11} Disulfide bonds are critical for folding as well as the thermodynamic and mechanical stability of many proteins.^{10,12–14} In the presence of reducing agents, the rate of disulfide reduction can be conveniently measured using single-molecule force-clamp spectroscopy.^{15,16}

Force-clamp spectroscopy is a novel technique for studying the conformational dynamics of single bonds during a chemical reaction.^{16,17} A force-clamp trace measures the time evolution of the end-to-end length of a molecule stretched by a constant force between the AFM tip and the substrate. In particular, single disulfide bond reduction events are accurately detected from the force-clamp traces as stepwise increases in the length of a polyprotein stretched in the presence of reducing agents.

In force-clamp studies of disulfide bond reduction, the reaction rate constant has been obtained by fitting a single exponential to the ensemble average of several force-clamp traces collected at a given force.¹⁶ Although providing a good first approximation for the reaction rate as a function of force and reagent concentration, a single-exponential fit presupposes only one process in the system. Using single-exponential fits to the

[†] Part of the Molecular and Surface Forces special issue.

* Corresponding authors. (R.S.) E-mail: rs2697@columbia.edu. (J.M.F.) E-mail: jfernandez@columbia.edu.

[‡] Columbia University.

[§] Universidad de Granada.

(1) Bustamante, C.; Chemla, Y. R.; Forde, N. R.; Izhaky, D. *Annu. Rev. Biochem.* **2004**, *73*, 705–48.

(2) Beyer, M. K.; Clausen-Schaumann, H. *Chem. Rev.* **2005**, *105*, 2921–48.

(3) Dufrene, Y. F. *Nat. Rev. Microbiol.* **2004**, *2*, 451–460.

(4) Molloy, J. E.; Padgett, M. J. *Contemp. Phys.* **2002**, *43*, 241–258.

(5) Ritort, F. *J. Phys.: Condens. Matter* **2006**, *18*, R531–R583.

(6) Dudko, O. K.; Mathe, J.; Szabo, A.; Meller, A.; Hummer, G. *Biophys. J.* **2007**, *92*, 4188–4195.

(7) Kinosita, K.; Shiroguchi, K.; Ali, M. Y.; Adachi, K.; Itoh, H. *Adv. Exp. Med. Biol.* **2007**, *592*, 369–384.

(8) Bakajin, O. B.; Duke, T. A. J.; Chou, C. F.; Chan, S. S.; Austin, R. H.; Cox, E. C. *Phys. Rev. Lett.* **1998**, *80*, 2737–2740.

(9) Szymczak, P.; Cieplak, M. *J. Chem. Phys.* **2006**, *125*, 164903.

(10) Thornton, J. M. *J. Mol. Biol.* **1981**, *151*, 261–287.

(11) Matthias, L. J.; Yam, P. T. W.; Jiang, X. M.; Vandegraaff, N.; Li, P.; Pombourios, P.; Donoghue, N.; Hogg, P. *J. Nat. Immunol.* **2002**, *3*, 727–732.

(12) Lide, D. R., Ed. *CRC Handbook of Chemistry and Physics*; CRC Press: Cleveland, OH, 1995.

(13) Cohen, C. J.; Li, Y. F.; El-Gamil, M.; Robbins, P. F.; Rosenberg, S. A.; Morgan, R. A. *Cancer Res.* **2007**, *67*, 3898–3903.

(14) Orenco, C. A.; Todd, A. E.; Thornton, J. M. *Curr. Opin. Struct. Biol.* **1999**, *9*, 374–382.

(15) Ainavarapu, R. K.; Brujic, J.; Huang, H. H.; Wiita, A. P.; Lu, H.; Li, L. W.; Walther, K. A.; Carrion-Vazquez, M.; Li, H. B.; Fernandez, J. M. *Biophys. J.* **2007**, *92*, 225–233.

(16) Wiita, A. P.; Ainavarapu, S. R. K.; Huang, H. H.; Fernandez, J. M. *Proc. Natl. Acad. Sci. U.S.A.* **2006**, *103*, 7222–7227.

(17) Fernandez, J. M.; Li, H. B. *Science* **2004**, *303*, 1674–1678.

ensemble average of force-clamp traces, we found a single reaction mechanism for a small-molecule reducing agent¹⁶ and two separate reaction mechanisms for the disulfide reduction catalyzed by the complex enzyme thioredoxin (TRX).¹⁸ However, density functional theory calculations have shown the possible existence of multiple transition states for disulfide bond reduction by a simple thiol reducing agent.¹⁹ Given these findings, there could be a multitude of transition states leading to different rates both in the case of the small-molecule reducing agent and the enzyme. Clearly, a method of fitting a single exponential to averaged ensemble kinetic traces cannot discern these multiple reaction mechanisms. How could these be identified? One option could be to fit these averaged single-molecule recordings with a multiexponential function, but fitting many exponentials usually allows for some degree of ambiguity (i.e., a given set of experimental data can always be better fitted with multiple exponentials, but their physical meaning is not clear unless additional criteria are applied).

Similar issues have been encountered in the widely used patch-clamp studies of single ion channels, which typically record the current flowing through a single channel as a function of an applied, constant voltage. In these studies, the macroscopic kinetics of channel opening and closing can be obtained by creating an ensemble of single-channel recordings and fitting these traces with a single- or multiple-exponential function.²⁰ To avoid the potential pitfalls of exponential fitting, dwell time histogram techniques, a more powerful method to measure reaction kinetics, have also been used.²⁰ For ion channels, these histograms are constructed by measuring the duration of time when the channel is in a given state, for example, in the “open” or “closed” state. It has been shown that logarithmic histograms of these dwell times can discriminate between various microscopic rates.^{21,22} Using logarithmic histograms with a square root ordinate versus a logarithmic time axis, Sigworth and Sine showed that the rate constants are unambiguously obtained in the case of a large number of events (approximately several thousand) and without invoking any further approximations.²²

Here, we investigate the issues of complexity and multiple reaction pathways in the context of single-molecule mechanochemistry. We use single-molecule force-clamp AFM spectroscopy to probe in detail the kinetics of single disulfide bond reduction in the protein (I27_{SS})₈ under a calibrated pulling force. We have obtained a large data set of single disulfide reduction events under force (4488 events) using two different reducing compounds: the phosphine-based small molecule TCEP (tris-(2-carboxyethyl)phosphine) and the enzyme thioredoxin, which are expected to differ in the complexity of their disulfide reduction mechanisms. First, we use exponential fits to ensemble averaged recordings together with a bootstrapping method to obtain the reaction kinetics from our single-molecule force-clamp experiments. Next, we use dwell time analysis and find that two reaction pathways are present in the case of TRX but only a single process is resolvable in the case of TCEP. We discuss the results in the context of the available kinetic models and resolution of the used techniques. Our results and analytical approaches advance the potential use of force-clamp spectroscopy in resolving chemical reactions under mechanical force.

Materials and Methods

Proteins and Chemicals. The expression and purification of the protein (I27_{G32C-A75C})₈, called here (I27_{SS})₈, has been described previously.¹⁶ Briefly, we used the QuikChange site-directed mutagenesis method (Stratagene) to introduce Gly32Cys and Ala75Cys mutations into the I27 module from human cardiac titin. We used multiple rounds of successive cloning to create an N–C-linked, eight-domain polyprotein gene, (I27_{G32C-A75C})₈.²³ This gene was encoded in vector pQE30 and expressed in *E. coli* strain BL21-(DE3). Pelleted cells were lysed by sonication, and the His₆-tagged protein was purified using first an immobilized Talon-Co²⁺ column (Clontech) and next by gel filtration on a Superdex 200 column (GE Healthcare). The purified protein was verified by SDS-PAGE and stored at 4 °C in a buffer of 10 mM HEPES, 150 mM NaCl, 1 mM EDTA, and 0.02% NaN₃ (w/v) at pH 7.2.

Wild-type TRX was expressed and purified as has been described by Perez-Jimenez et al.²⁴ Briefly, the *E. coli* TRX gene, encoded in plasmid pTK100, was expressed in *E. coli* strain JF521. Cell pellets were lysed using a French press and stirred with streptomycin sulfate (10% w/v) at 4 °C overnight. The filtered supernatant was then loaded onto a 2-L Sephacryl S-100 high-resolution (GE Healthcare) gel filtration column. TRX fractions were pooled and applied to a 250 mL Fractogel EMD DEAE(M) (Merck) ion exchange column equilibrated in 1 mM EDTA and 30 mM TRIZMA buffer at pH 8.3. The protein was eluted by a linear gradient between 0 and 0.5 M NaCl. SDS-PAGE gel densitometry confirmed the proteins' purity. The molecular weight of pure proteins was confirmed by mass spectrometry. TRX fractions were dialyzed into a buffer of 10 mM HEPES, 150 mM NaCl, and 1 mM EDTA at pH 7.2. The TRX concentration was determined spectrophotometrically at 280 nm using an extinction coefficient ϵ_{280} of 13 700.

TCEP·HCl powder was purchased from Sigma and used without further purification, and a 2.5 mM solution of TCEP was prepared in the PBS buffer and titrated with 1 M NaOH to pH 7.2. For experiments with thioredoxin, we used a buffer containing 12 μ M TRX, 10 mM HEPES buffer, 150 mM NaCl, 1 mM EDTA, 2 mM NADPH, and 50 nM of thioredoxin reductase from *E. coli* (purchased from Sigma), titrated with 1 M NaOH to pH 7.2. Excess NADPH and a catalytic amount of thioredoxin reductase are both necessary to maintain ~98% of TRX in the active, reduced form during the experiment.²⁵

Force-Clamp AFM Spectroscopy. Our custom-built AFM setup uses a modified AFM head from Multimode AFM (Veeco), an external laser source (SK9733C, Schaefer, Germany), a PicoCube XYZ scanner (P363.3-CD, Physik Instrumente, Germany), and custom electronics equipped with a standard analog proportional, integral, and differential feedback circuits. Data acquisition and data analysis routines have been developed under Igor Pro 5.0 (Wave-metrics). The raw data is filtered with a 200 Hz low-pass filter to distinguish between unfolding and reduction events easily. We use commercial V-shaped silicon nitride AFM cantilevers (MLCT-Au, type C, from Veeco), with their normal elastic spring constants k_N calibrated in liquid, prior to each experiment, by a thermal method.²⁶ The mean value of k_N , averaged over 52 cantilevers reported in this study (17 experiments for TCEP and 35 experiments for TRX), is 15.2 ± 3.9 pN/nm (standard deviation). We use a standard DI MultiMode quartz liquid cell with a silicon O-ring around it to reduce thermal drifts and to keep the concentration of reducing agents constant throughout each experiment. Gold-coated standard microscope cover slides (Fisher Scientific) are used as a substrate. We use only between 5 and 8 μ L of a protein solution for each AFM experiment. This keeps the probability of picking a single protein

(18) Wiita, A. P.; Perez-Jimenez, R.; Walther, K. A.; Grater, F.; Berne, B. J.; Holmgren, A.; Sanchez-Ruiz, J. M.; Fernandez, J. M. *Nature* **2007**, *450*, 124–127.

(19) Fernandes, P. A.; Ramos, M. J. *Chem.—Eur. J.* **2004**, *10*, 257–266.

(20) Hamill, O. P.; Marty, A.; Neher, E.; Sakmann, B.; Sigworth, F. J. *Pflügers Arch.* **1981**, *391*, 85–100.

(21) Blatz, A. L.; Magleby, K. L. *J. Physiol. (London, U.K.)* **1986**, *378*, 141–174.

(22) Sigworth, F. J.; Sine, S. M. *Biophys. J.* **1987**, *52*, 1047–1054.

(23) Carrion-Vazquez, M.; Oberhauser, A. F.; Fowler, S. B.; Marszalek, P. E.; Broedel, S. E.; Clarke, J.; Fernandez, J. M. *Proc. Natl. Acad. Sci. U.S.A.* **1999**, *96*, 3694–9.

(24) Perez-Jimenez, R.; Godoy-Ruiz, R.; Ibarra-Molero, B.; Sanchez-Ruiz, J. M. *Biophys. Chem.* **2005**, *115*, 105–107.

(25) Holmgren, A. *Annu. Rev. Biochem.* **1985**, *54*, 237–71.

(26) Florin, E. L.; Rief, M.; Lehmann, H.; Ludwig, M.; Dornmair, K.; Moy, V. T.; Gaub, H. E. *Biosens. Bioelectron.* **1995**, *10*, 895–901.

low (roughly 1% of the trials) but increases the chances of picking only one molecule at a time.

On the basis of trial experiments, our choice of forces and clamp times meets the following criteria: (i) to unfold a protein quickly but still be able to resolve its unfolding steps, (ii) to provide a minimum lag time between unfolding and first reduction, and (iii) to clamp (I27_{SS})₈ long enough to collect very slow reduction events and not to skew the statistics by storing only the fast traces. Any significant changes in the protein end-to-end length occur only after the molecule has been picked up from the surface and elastically stretched over a distance of tens of nanometers. Thus, the kinetics of disulfide reduction should depend neither on the water structure at the surface²⁷ nor on the elastoadhesive properties of the contacting asperities among the AFM tip, the protein, and the substrate.²⁸ We have never observed $-S-S-$ cleavage in the absence of reducing agents.¹⁶ This result is expected given the results of Grandbois *et al.*,²⁹ where it has been shown that forces greater than 1 nN are required to rupture a covalent bond and the contact between the tip/protein/substrate typically breaks below 1 nN.¹⁵

Our AFM is mechanically isolated by the standard pneumatic table and an active mechanical damping system (Minus K from NanoK). Thus, the drift in the force-clamp data comes chiefly from thermal gradients within a cantilever, in a solution, and in a piezotransducer. To minimize drift, we typically wait for at least 20–30 min before starting data collection and readjust the AFM feedback if needed.

Data Analysis. We use the standard statistical Pearson test to assess the goodness of fitting a given trend to the experimental data set. This test is based on calculating the χ^2 value, $\chi^2 = \sum_i (y_i - f(x_i))^2 / \sigma^2$, where \sum_i is the sum over the fitted data points, y_i is the experimental value at the i th point (e.g., the value of a histogram at the i th bin), $f(x_i)$ is the value of a fitted function at the i th point (e.g., the probability density function in the case of a histogram), and σ is the standard deviation of a fit. To differentiate unambiguously between different models, the reduced χ_{red}^2 , $\chi_{red}^2 = \chi^2 / (N - c)$, is often reported, where N is the number of fitted data points, c is the number of constraints, and the value of $\chi_{red}^2 < 1$ signifies a good fit.

In the dwell time analysis, the rate constants for the disulfide reduction are obtained from the linear and logarithmic histograms of the dwell times through the fits of a functional form of the histogram's ordinate. The ordinate y of the linear histogram is number of events n_i in each bin: $y = n_i = N \delta t f(x)$, where N is the total number of events, δt the bin size, and $f(t)$ is the probability density function. In the case of a multiple exponential series, the value of $f(t)$ is $f(t) = \sum_i a_i \exp(-tk_i + \delta t/2)$, where t is the time, a_i is the normalized fraction of N , and \sum_i is the sum over all of the wanted rate constants k_i . The ordinate of the logarithmic histograms used here is the square root of the number of events: $y = n_i^{1/2} = (N \delta x g(x))^{1/2}$.²² The corresponding probability density function is $g(x) = \sum_i a_i \exp(x + \ln(k_i) + \delta x/2 + \exp(x + \ln(k_i) + \delta x/2))$, where $x = \ln(t)$ is the logarithmic abscissa and δx is the bin size (constant on the log scale).

In the dwell time analysis, a small bin size improves the detection of the rate constants, but bins that are too narrow are unphysical because the number of events within them is too small. To determine a proper bin size, we use a χ^2 test while fitting the histogram's ordinate. In our procedure, the bin size gradually increases from an arbitrarily small value until the value of χ^2 decreases to the vicinity of its global minimum. In linear histograms, σ is the square root of the ordinate. In logarithmic histograms, $\sigma = 0.5$ for each bin.²² In the case of linear histograms, a bin size of 0.3 s has been chosen. In the case of the logarithmic histograms, a uniform δx value of 0.34 for both TCEP and TRX has been set.

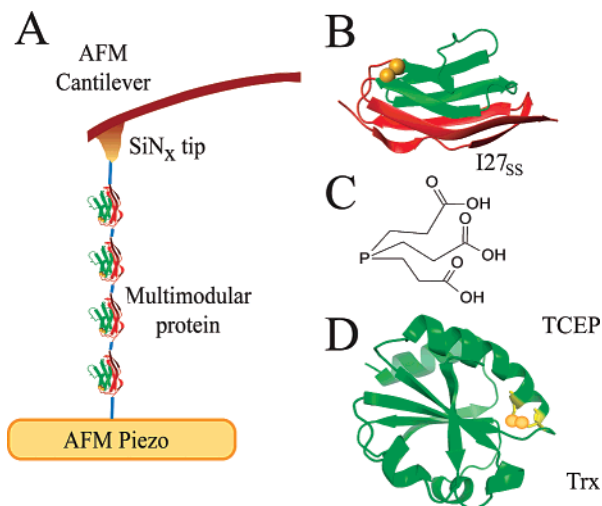


Figure 1. Experimental setup. (A) In the AFM force spectroscopy setup, the silicon nitride cantilever picks up, extends, and keeps under a constant force a single polyprotein. (B) One module of (I27_{SS})₈ is an octamer polyprotein composed of the I27 domain of cardiac titin with one disulfide bond formed between residues 32 and 75 (yellow spheres). The residues in green are mechanically “trapped” behind the disulfide bond, whereas the residues in red will be exposed to a pulling force applied to the protein N and C termini. In our experiments, the disulfide bonds in (I27_{SS})₈ are reduced one at a time. To accomplish disulfide reduction, we use the following reducing agents: (C) a phosphine-based nucleophile, tris-(2-carboxyethyl)phosphine hydrochloride (TCEP), and (D) a biological enzyme, thioredoxin (TRX), containing catalytic cysteines (yellow) to reduce disulfide bonds via their thiol groups (yellow spheres).

Our bootstrapping method takes the longest trace (36 s) as a time reference and extends all shorter force-clamp traces to this time using a constant-length value identical to that just before detachment. This method assumes, according to our experimental criteria, that no reduction events occur in the extended portion of the traces.

Experimental Results

Identifying Disulfide Reduction Events. In the force-clamp mode (Figure 1), the AFM tip taps and rasters the substrate's surface in an attempt to pick up single molecules of the octameric polyprotein (I27_{SS})₈ (Figure 1b). During each trial, the following experimental protocol is repeated. Initial tip–sample contact is maintained by standard AFM feedback for 1 s with a static setpoint force of 1 nN. Next, the setpoint force is reduced to 100 pN and maintained for 100 ms. If a polyprotein (or a portion of it) gets trapped between the tip and the sample, then this point arbitrarily defines its zero extended end-to-end length on the force-clamp trace (Figure 2b). The (I27_{SS})₈, where each domain contains a sequestered disulfide bond, is then pulled at 190 pN for 0.2 s in order to partially unfold this protein and expose the buried disulfide bonds to the bathing solution with the reducing agent (Figure 2a). Next, a force of 180 pN (in the case of TCEP) or 100 pN (in the case of TRX) clamps (I27_{SS})₈ for an additional 36 s. We chose these two clamping forces to result in similar overall rates for each type of reducing agent, facilitating comparison between the two agents on similar time scales. The particular force values were chosen on the basis of our previous results on TRX,¹⁸ previous experiments with TCEP,³⁰ and trial experiments.

We have used two disulfide bond reducing agents: TCEP, a simple chemical reducing agent (Figure 1c), and thioredoxin from the bacteria *E. coli* (Figure 1d). TCEP is a phosphine-based nucleophile, and when compared to common sulfur-based reducing agents such as dithiothreitol (DTT), it is less toxic and more stable at room temperature.³¹ TRX is a globular enzyme found in all living

(27) Li, T. D.; Gao, J. P.; Szozkiewicz, R.; Landman, U.; Riedo, E. *Phys. Rev. B* **2007**, *75*, 115415.

(28) Szozkiewicz, R.; Kulik, A. J.; Gremaud, G.; Lekka, M. *Appl. Phys. Lett.* **2005**, *86*, 014310.

(29) Grandbois, M.; Beyer, M.; Rief, M.; Clausen-Schaumann, H.; Gaub, H. E. *Science* **1999**, *283*, 1727–30.

(30) Ainavarapu, S. R. K.; Wiita, A. P.; Uggerud, E.; Fernandez, J. M. submitted for publication, 2007.

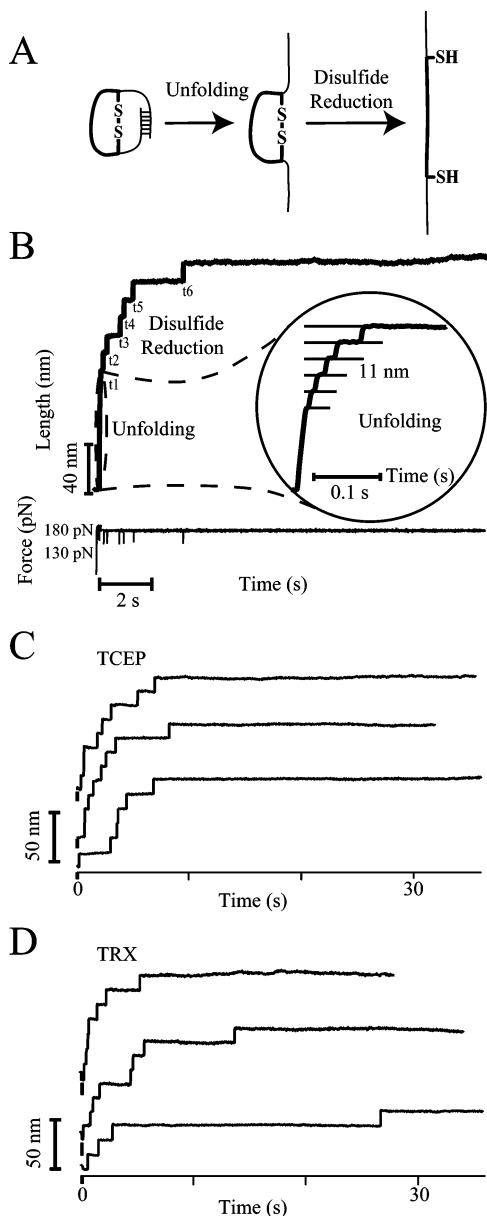


Figure 2. Identifying single disulfide reduction events in force-clamp spectroscopy. (A) Under a stretching force, each module of $(I27_{SS})_8$ (shown in Figure 1) partially unfolds up to the mechanically strong disulfide bond. This bond is buried in the folded protein and is not exposed to the solution until mechanical unfolding occurs. If a reducing agent is present in solution, then the disulfide bond can be reduced, and the “trapped” residues will be rapidly extended. (B) A sample force-clamp trace (obtained in the presence of 2.5 mM TCEP) measures the $(I27_{SS})_8$ end-to-end extended length as a function of time. During the first 200 ms at a pulling force of 190 pN, the protein first extends elastically, and then many modules unfold up to the disulfide bond. Five unfolding steps, each resulting in a length increase of ~ 11 nm, are clearly resolvable (inset). After exposing the disulfide bond to the solvent, the reduction of single disulfide bonds can be recorded as a function of time at 180 pN (the trace with six ~ 14 nm steps). By analogy to single ion channel recordings, the times at which single disulfide reduction events occur following the unfolding pulse are called dwell times, and these dwell times are indicated by $t_1 \dots t_6$. A few further examples of the force-clamp trace recordings showing only the portion of the trace following unfolding and containing the disulfide reduction are presented in part C for 2.5 mM TCEP with a clamping force of 180 pN and in D for 12 μ M TRX with a clamping force of 100 pN.

organisms. TRX plays a critical role in disulfide bond reduction, maintenance of redox homeostasis, anti-apoptotic activity, and signaling.^{25,32}

The unfolding of each module up to the disulfide bond, at 190 pN, yields 10.7 ± 1.1 nm steps in the end-to-end length of the protein. Correspondingly, each reduction event yields 14.1 ± 1.4 nm steps at 180 pN and 13.1 ± 1.3 nm steps at 100 pN. This fingerprint allows the reduction events and the initial partial unfolding events to be easily recognized and distinguished from one another and from any other spurious events. We also discard the traces with an occasional unfolding step intercalating the pattern of reduction steps because our aim here is to study the kinetics of disulfide reduction and not the kinetics of unfolding.

Ensemble Kinetic Analyses of Disulfide Reduction. The kinetics of the single-molecule disulfide bond reduction events is illustrated in Figure 2b, which presents a typical force-clamp trace obtained in the presence of TCEP. Rate constants can be obtained from an average of several force-clamp traces by fitting exponentials.¹⁶ This type of summation and fitting has been used extensively in the ion channel literature,^{33,34} so it is a good starting point for our analysis.

To obtain the averaged force-clamp trace, we sum and normalize the total collected set (master set) of 425 force-clamp traces for TCEP or 726 force-clamp traces for TRX. The end-to-end protein length is normalized to the total number of reduction events (i.e., 1513 events for TCEP and 2975 for TRX). After examining several force-clamp traces, we have found the onset time for each reduction step within ~ 1 ms, even though sampling gives us a time resolution as high as 200 μ s. Thus, we interpolate the time axis with equally spaced (1 ms) data points. To obtain the reduction rate constants we fit the averaged trace with (a) single- and (b) double-exponential functions as illustrated in Figure 3. We present the resulting rate constants and their amplitudes in Table 1 (for TCEP) and in Table 2 (for TRX) under the heading “ensemble average”.

The results of the averaged ensemble of force-clamp recordings show that in the case of TRX the fit residuals improve significantly in a double-exponential model when compared to the single-exponential fit (Figure 3d). However, the improvement is much less prominent in the case of TCEP (Figure 3b). A similar trend is observed for the χ_{red}^2 (reduced χ^2) values (Tables 1 and 2), which represent the overall fit quality as described in detail in Materials and Methods. The errors in the obtained rate constants and their amplitudes are small, which seems to be mostly due to the large number of data points even after the time interpolation procedure.

To estimate the standard errors in the measured rate constants, we use the bootstrapping method.³⁵ In our bootstrapping analysis, a random subset of force-clamp traces is drawn with replacement from the master data set of 425 force-clamp traces for TCEP or 726 force-clamp traces for TRX. This random subset contains the same total number of traces as the original data set, but some traces may be included multiple times and others are not included at all. Each subset is averaged and fit by a single- or double-exponential function. This procedure is repeated 2000 times, generating 2000 subsets and a corresponding number of rate constants from the exponential fit functions. These rate constants occur with varying frequency, and their distributions for the double-exponential fits are plotted in Figure 4. The mean values of the rate constant distributions for both the single- and double-exponential fits are shown in Tables 1 and 2 under “bootstrapping”. The standard deviation for each rate constant distribution is equal to the standard error of the mean for the master set of force-clamp recordings.³⁵

In Figure 4, the peak at a higher rate for TCEP (i.e., 1.05 s^{-1}) is much more spread out than other peaks, indicating that this rate is not as well defined as in the case of TRX. Similar to the ensemble-averaged analyses, the results of bootstrapping suggest that a single-exponential fit works well in the case of TCEP and a double-exponential fit works better in the case of TRX. However, it would seem desirable to compare these results with a different method of finding the reaction kinetics from the force-clamp experiments.

(31) Burns, J. A.; Butler, J. C.; Moran, J.; Whitesides, G. M. *J. Org. Chem.* **1991**, *56*, 2648–2650.

(32) Arner, E. S.; Holmgren, A. *Eur. J. Biochem.* **2000**, *267*, 6102–6109.

(33) Sigworth, F. J.; Neher, E. *Nature* **1980**, *287*, 447–449.

(34) Aldrich, R. W.; Corey, D. P.; Stevens, C. F. *Nature* **1983**, *306*, 436–441.

(35) Efron, B. *The Jackknife, the Bootstrap, and Other Resampling Plans*; SIAM: Philadelphia, PA, 1982.

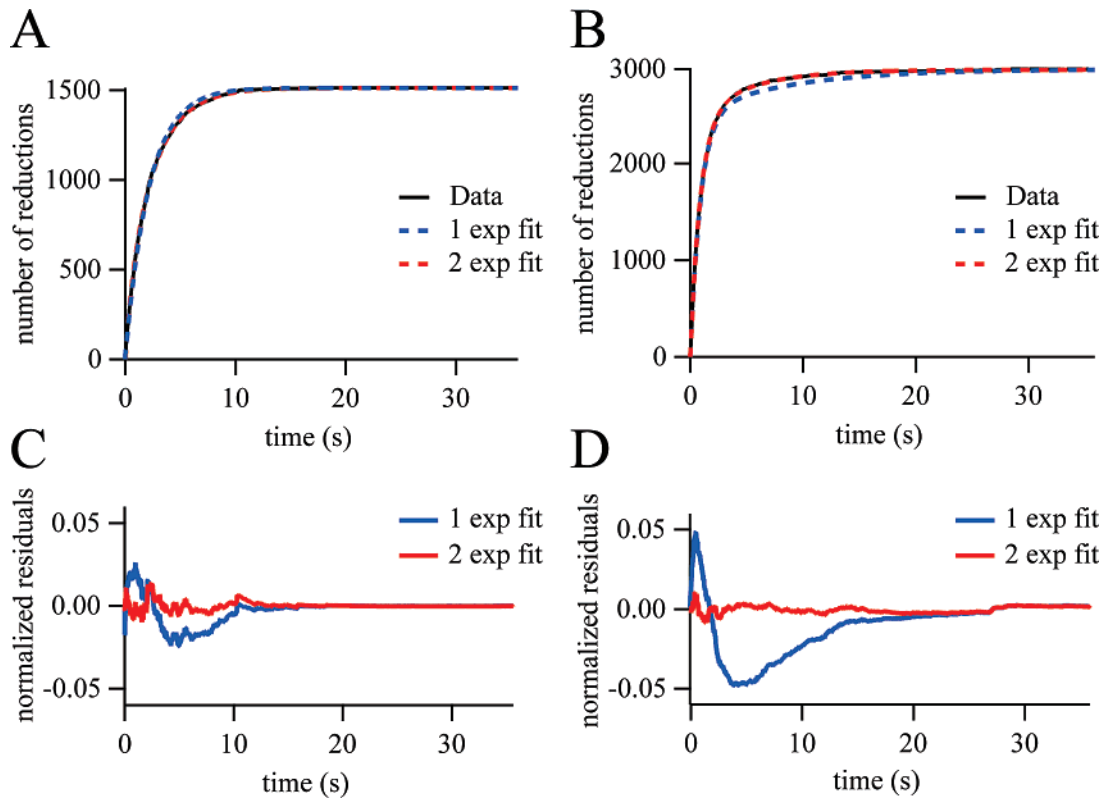


Figure 3. Exponential fits to the ensemble average of force-clamp recordings. (A) 425 AFM force-clamp traces for TCEP and (B) 726 AFM force-clamp traces for TRX are summed and normalized to the cumulative number of reduction events. The resulting traces are equivalent to a probability distribution function for reduction and are fitted with both a single and a double exponential to obtain the ensemble reduction kinetics. The normalized residuals of these fits are presented in part C for TCEP and in part D for TRX. The fit parameters are presented in Table 1 (for TCEP) and Table 2 (for TRX).

Table 1. Results of Statistical Analyses for TCEP

TCEP	ensemble average	bootstrapping	linear histograms	logarithmic histograms
single-exponential rate constant (s^{-1})	0.47 ± 0.02	0.44 ± 0.02	0.47 ± 0.02	0.45 ± 0.02
χ_{red}^2	0.3^a		0.7^a	0.9^a
double exponential				
rate constant ₁ (s^{-1})	0.39 ± 0.01	0.37 ± 0.03	0.40 ± 0.10	0.38 ± 0.03
amplitude ₁ (events) [% of total]	1252.8 ± 12.6 [83%]	40.72 ± 5.93 [75%]	120.8 ± 84.6 [55%]	1118.4 ± 203 [74%]
rate constant ₂ (s^{-1})	1.51 ± 0.16	1.21 ± 0.53	0.94 ± 0.54	1.00 ± 0.32
amplitude ₂ (events) [% of total]	263.2 ± 11.3 [17%]	13.50 ± 5.79 [25%]	98.7 ± 81.3 [45%]	394.6 ± 203 [26%]
χ_{red}^2	0.1		0.5	0.6

^a Increased exponential does not improve the fit.

Table 2. Results of Statistical Analyses for TRX

TRX	ensemble average	bootstrapping	linear histograms	logarithmic histograms
single-exponential rate constant (s^{-1})	0.84 ± 0.01	0.73 ± 0.03	0.88 ± 0.02	0.74 ± 0.08
χ_{red}^2	1.1		1.9	14
double exponential				
rate constant ₁ (s^{-1})	0.21 ± 0.01	0.19 ± 0.03	0.30 ± 0.06	0.16 ± 0.01
amplitude ₁ (events) [% of total]	533.1 ± 5.8 [18%]	0.17 ± 0.03 [17%]	45.4 ± 19.6 [7%]	537.4 ± 43.4 [18%]
rate constant ₂ (s^{-1})	1.13 ± 0.01	1.09 ± 0.05	1.12 ± 0.06	1.08 ± 0.03
amplitude ₂ (events) [% of total]	2436.7 ± 5.9 [82%]	0.83 ± 0.03 [83%]	654.2 ± 23.8 [93%]	2437.6 ± 43.4 [82%]
χ_{red}^2	0.1^a		0.7^a	0.8^a

^a Increased exponential does not improve the fit.

Dwell Time Analysis of Disulfide Reduction. Dwell time analysis has been widely used in the ion channel community to investigate reaction kinetics from single ion channel recordings. By analogy, we define the dwell time as the time duration until a given reduction event occurs, counting from the time when the given disulfide bond

has been exposed to the reducing agent. Here, the zero time is set at the end of the initial 200 ms allotted for (I27_{SS})₈ unfolding, and the dwell times are measured as the difference between the zero time and the times taken at the onset of the reduction steps (Figure 2). We have extracted the dwell times from the force-clamp traces by

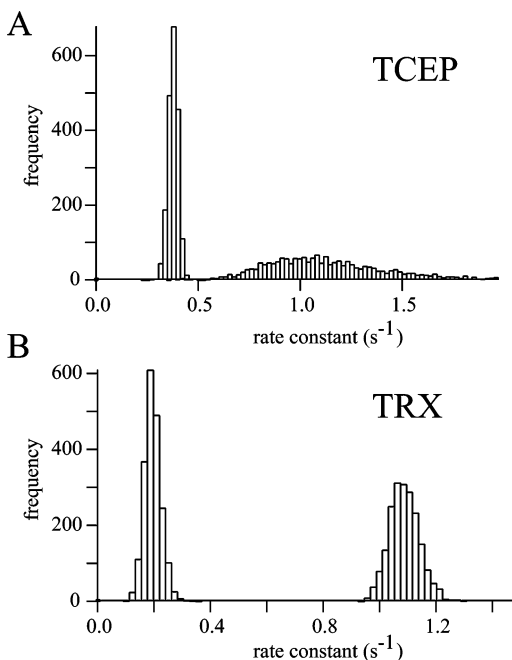


Figure 4. Bootstrapping. In this method, a set of 425 traces for TCEP and 726 AFM traces for TRX is randomly chosen with replacement and averaged from their respective master data sets of the same size. Each set of randomly chosen traces is fitted by a double-exponential function (similar to Figure 3), and the procedure is repeated 2000 times, resulting in a distribution of the fitted rate constants. In part A, the results of the double-exponential fit for TCEP are presented. There are 2000 fits for each rate so that the area under each peak is the same. The mean values along with their standard error are shown in the Table 1. One can see that the second component at 1.05 s^{-1} is blurred, indicating that TCEP has only one well-defined reaction mechanism. Part B presents a similar analysis for TRX. The two peaks are now sharp and well-defined. Their mean values and standard deviations are shown in Table 2.

means of a step detection algorithm (Supporting Information). As mentioned before, the uncertainty in detecting the onset of each reduction step is 1 ms, and this value also sets the minimum detectable dwell time. To obtain information about the kinetics of disulfide reduction, the dwell times are displayed in the form of a histogram. Each dwell time produces an event in the histogram.

In Figure 5, we plot the linear histograms of the dwell times for all 1513 events collected for TCEP and 2975 events collected for TRX. The optimal bin size for these histograms has been determined on the basis of a χ^2 analysis as explained in Materials and Methods. Visually, the linear histograms do not offer much information about the underlying kinetic processes for each reducing agent. For TRX, it is apparent that a few events are scattered at longer times ($> 10 \text{ s}$) but the majority of events cluster below 1 s for both TCEP and TRX.

The rate constants for the disulfide reduction are typically obtained from the probability density functions fitted to a given histogram. We have fitted (a) a single-exponential and (b) a double-exponential form of the probability density function to these histograms and have calculated χ_{red}^2 as explained in detail in Materials and Methods. Errors in the rate constants result from the fit error. We report the obtained results in Table 1 for TCEP and in Table 2 for TRX under the column heading "linear histograms". On the basis of the common criterion in the statistical Pearson test, where $\chi_{\text{red}}^2 < 1$ signifies a good fit, we deduce that a single-exponential fit does well in the case of TCEP and a double-exponential fit does well in the case of TRX but the single- and double-exponential fits do not differ much in these histograms.

The exponential fits to ensemble-averaged data, bootstrapping, and the linear histograms of dwell times do not visually distinguish between the kinetics of several different processes. In the ion channel community, these problems have been addressed by utilizing a type

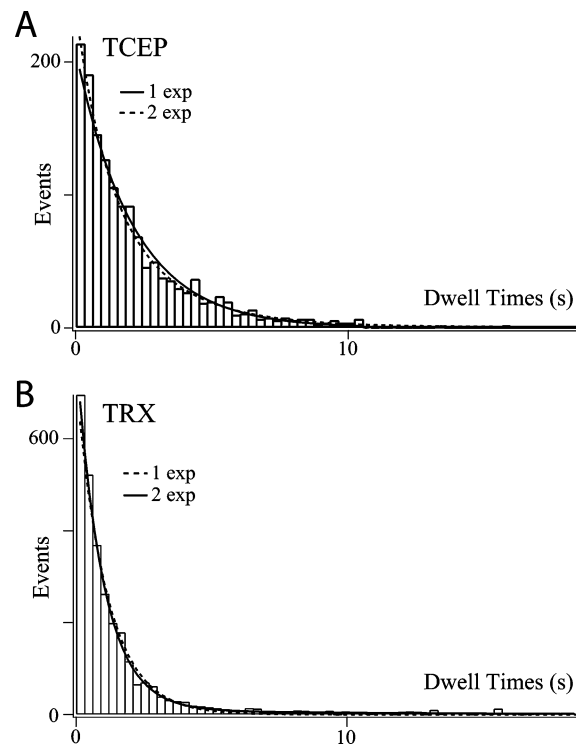


Figure 5. Linear histograms of dwell times. (A) The dwell times are gathered in the linear histograms in the case of TCEP and (B) in the case of TRX. The histograms are fitted with single- and double-exponential functions, and the results are presented in Table 1 (for TCEP) and Table 2 (for TRX).

of logarithmic histograms displaying the square root of events versus the logarithm of the dwell times (see Materials and Methods for details).²² These logarithmic histograms have several advantages: (i) each rate constant gives a peak in the histogram; (ii) any change in the rate constant produces only a horizontal shift of the histogram rather than a change of scale; and finally (iii) assuming Poisson statistics, the errors are evenly distributed for each bin.

Figure 6 shows the logarithmic histograms in the cases of TCEP (Figure 6a) and TRX (Figure 6b). The bin sizes of these histograms have been chosen in the iterative procedure described in Materials and Methods. These histograms show single-exponential kinetics for TCEP and double-exponential kinetics for TRX. In the case of TCEP, we obtain a rate constant of $0.45 \pm 0.01 \text{ s}^{-1}$. In the case of TRX, we obtain two rate constants of 1.08 ± 0.03 and $0.16 \pm 0.01 \text{ s}^{-1}$, with their amplitude ratio of 4.54 ± 0.41 for TRX. The dwell time analysis using logarithmic histograms clearly seems to be appropriate for displaying the kinetics of the single-molecule disulfide bond reductions obtained by force-clamp spectroscopy. The various processes are well represented, and their relative amplitude ratio can be easily calculated. These results provide further evidence for the different chemistry occurring in disulfide reduction by a small molecule and that catalyzed by an enzyme. The implications of these findings are discussed below.

Discussion

Comparisons between the Analysis Results for Disulfide Reduction. In the ensemble kinetics analyses both for TCEP and TRX, we have noticed that an increased number of exponentials fit the experimental data better. It is therefore imperative to incorporate additional criteria to distinguish when more exponentials are justified. The goodness of these fits can be quantified by calculating the rate integrals. The i th component of the rate integral is given by $I_i = \int dt A_i \exp(-k_i t) = A_i/k_i$, where A_i is the amplitude of the i th component I_i , k_i is its rate constant, and t is the time. In the case of TCEP, the contribution of the predominant rate integral at 0.39 s^{-1} is $\sim 95\%$ for the

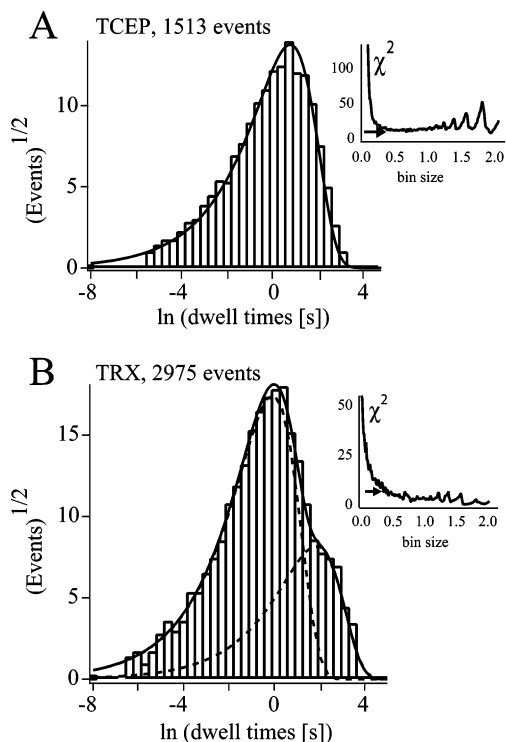


Figure 6. Logarithmic histograms of dwell times. (A) For TCEP and (B) for TRX, the square root ordinate of the number of dwell times (events) are displayed as a function of the logarithm of the dwell times. (See Materials and Methods for details.) In the case of TCEP, we obtain a single rate constant of $0.45 \pm 0.01 \text{ s}^{-1}$. In the case of TRX, we obtain two rate constants of 1.08 ± 0.03 and $0.16 \pm 0.01 \text{ s}^{-1}$, with an amplitude ratio of 4.54 ± 0.41 (dashed lines for each exponential process, solid line for the total fit). In the insets, we present how χ^2 analysis was used to choose the optimal bin size for these histograms. The histograms with varying bin sizes were fitted by their probability density functions until the calculated χ^2 for a given fit decreased to its first minimum (Materials and Methods). This analysis resulted in very similar bin sizes for both TCEP and TRX, allowing for easy comparison between the two reducing agents.

ensemble-averaging approach (whereas its corresponding normalized amplitude is 83%; Table 1). Using typical criteria, any component contributing less than 10% is usually ignored,³⁶ indicating that a single-exponential fit suffices to fit the TCEP data. For TRX, however, this same analysis shows that the use of two exponentials is justified, with the two components having rate integral contributions of 54% (0.21 s^{-1}) and 46% (1.13 s^{-1}). In Figure 4a, the bootstrapping analysis also shows that a possible additional, higher rate for TCEP is distributed over a wide range ($0.5\text{--}2 \text{ s}^{-1}$) and does not lead to a well-defined rate. This is in contrast to the sharp peaks observed for two separate rates in the TRX bootstrap analysis (Figure 4b). Furthermore, as mentioned above, the improvement in χ_{red}^2 is minimal in the case of TCEP with the addition of a second exponential, but in the case of TRX, a second exponential markedly improves the fit (Tables 1 and 2). Surely, the logarithmic histograms of the dwell times provide the clearest and most direct method of visualizing the reaction rates—the peaks in the logarithmic histograms correspond to the rate constants of the underlying kinetic processes—and no second peak is observed for TCEP.

We acknowledge that other, more complicated models could be incorporated into the analysis of rate constants. In particular, the continuous distribution of rates described by either normal, Lorentzian, or log-normal distribution functions could potentially

be applied.³⁷ In addition, the Kohlrausch stretched-exponential decay model is often used for non-single-exponential decay curves, and in the context of protein folding, power laws have recently been suggested.^{38–41} However, our experimental data seem to be well described by discrete exponential models, indicating no need for a more sophisticated analysis.

For each (I27_{SS})₈ molecule, there might be as many as eight reduction events. All of the presented methods of kinetic analysis assume that these single reduction events are independent from one another (i.e., the kinetics is Markovian). Similarly as in the paper by Brujic *et al.*,⁴² this assumption is verified (in Supporting Information) by two methods: (i) Monte Carlo simulations of the force-clamp traces and (ii) the ensemble kinetics fits to the two subsets of experimental data, with only two and with only seven reduction events per trace.

Are There Multiple Reaction Mechanisms for TCEP? The results of exponential fits to averaged data as well as the bootstrapping method indicate that there could be two reaction mechanisms for TCEP, with a small proportion of the reaction that proceeds through an alternate mechanism with a higher rate. The logarithmic histograms, however, show no visual evidence of such a second mechanism. Thus, it remains an open question as to whether multiple reaction pathways exist in the case of TCEP.

It has been proposed that TCEP reduces disulfide bonds via a bimolecular nucleophilic substitution (S_N2) mechanism.³¹ In this reaction, a phosphorus atom with a lone electron pair attacks one of the sulfur atoms in the disulfide bond, and a single transition complex is formed. This transition-state complex with elongated —P—S—S— bonds then converts to a quickly hydrolyzing phosphonium ion. In an uncomplicated S_N2 reaction, one would expect well-defined single-exponential kinetics in the time course of the average force-clamp trace. Furthermore, in such a two-state reaction with a single transition state, the dwell times in the linear histogram should be exponentially distributed as well as exhibit a single peak in the logarithmic histogram.

However, there might be more, but much less probable, processes occurring in disulfide bond reduction by simple chemical reducing agents such as TCEP.¹⁹ In the case of multiple reaction mechanisms, each transition state leads to a different single-molecule reaction rate. Under what circumstances would any other transition state become distinguishable in the force-clamp experiments?

Sine *et al.*,²² Carter *et al.*,⁴³ and Wachtel *et al.*⁴⁴ have approached the problem of resolving different transition states. Taking into account double-exponential kinetics with two mean rates r and r' of equal amplitude, they could still resolve only cases with $r/r' > 2.5$. Furthermore, their fitting errors have improved by only a factor of 3 with a 10-fold increase of the number of events, and the percentage of errors has increased hyperbolically once the amplitudes of r and r' started to be uneven or more distributions have been taken into account. Thus, even in the most extreme case with double-exponential kinetics and the same amplitude of r and r' , the minimum r/r' that could probably be resolved in our experiment is ~ 2.5 , which is on the order of the mathematical

(37) van Driel, A. F.; Nikolaev, I. S.; Vergeer, P.; Lodahl, P.; Vanmaekelbergh, D.; Vos, W. L. *Phys. Rev. B* **2007**, *75*, 035329.

(38) Kohlrausch, K. W. F. *Ann. Phys.* **1854**, *91*, 179.

(39) Włodarczyk, J.; Kierdaszuk, B. *Biophys. J.* **2003**, *85*, 589–598.

(40) Cieplak, M.; Hoang, T. X.; Li, M. S. *Phys. Rev. Lett.* **1999**, *83*, 1684–1687.

(41) Brujic, J.; Hermans, R. I.; Walther, K. A.; Fernandez, J. M. *Nature Phys.* **2006**, *2*, 282–286.

(42) Brujic, J.; Hermans, R. I. Z.; Garcia-Manyes, S.; Walther, K. A.; Fernandez, J. M. *Biophys. J.* **2007**, *92*, 2896–2903.

(43) Carter, A. A.; Oswald, R. E. *J. Neurosci. Methods* **1995**, *60*, 69–78.

(44) Wachtel, R. E. *J. Neurosci. Methods* **1988**, *25*, 121–128.

(36) Chithambo, M. L. *J. Phys. D: Appl. Phys.* **2007**, *40*, 1874–1879.

constant e (~ 2.7). In the case of unequal amplitudes of r and r' , which is likely to occur experimentally, the resolvable r/r' ratio is even higher.

The simple, yet widely used, Bell model can describe the effect of force on the mean rate r of a bimolecular chemical reaction.^{16,45} It reads

$$r = [\text{red}] \exp\left[\frac{-E_a + F\Delta x}{k_B T}\right] \quad (1)$$

In eq 1, [red] is the concentration of the reducing agent, E_a is the activation energy barrier, F is the force, and Δx is the distance to the transition state (in the sense of the reaction coordinate). Thus, for any two different transition states with corresponding mean rates r and r' , the ratio r/r' yields

$$\frac{r}{r'} = \exp\left[\frac{\Delta E_a - F\Delta\Delta x}{k_B T}\right] \quad (2)$$

where ΔE_a is the difference in activation energies between the two transition states and $\Delta\Delta x$ is the difference in the corresponding Δx . Ainaravaru et al.³⁰ has estimated that for TCEP, $E_a = 58.3 \pm 0.05$ kJ/mol and $\Delta x = 0.46 \pm 0.03$ Å. At $F = 180$ pN, $F\Delta x$ is only about 10% of E_a , and $F\Delta\Delta x$ should be even a significantly lower fraction of E_a so that $(\Delta E_a - F\Delta\Delta x) \approx \Delta E_a$.

On the basis of the aforementioned discussion, the resolvable ratio $r/r' \approx 2.5 \approx \exp(1)$, and on the basis of eq 2, $r/r' = \exp[-(\Delta E_a - F\Delta\Delta x)/k_B T] \approx \exp[(\Delta E_a)/k_B T]$. Thus, the detectable ΔE_a is on the order of $k_B T$, and this value is only about 1/20th of the estimated E_a for TCEP. This conclusion is important in light of the theoretical findings of Fernandes and Ramos.¹⁹ In their studies of disulfide bond reduction by a simple monothiol molecule, they found that the most likely reaction mechanism involved an uncomplicated bimolecular nucleophilic substitution (S_N2). However, they also studied the energetics of alternate transition states for disulfide reduction, including both different protonation states of the attacking sulfur as well as varying numbers of solvent molecules. They found that these other transition states typically required activation energies on the order of $(10-30)k_B T$ higher than for the uncomplicated S_N2 transition state. If these alternate reaction mechanisms play a major role in the reduction of disulfide bonds by TCEP, then we would expect to resolve them even if the amplitudes of r and r' for the two mechanisms are not equal. Thus, our results using the logarithmic histogram support the likelihood of only one predominant reaction mechanism for TCEP. We note, however, that we have thoroughly explored only one combination of a clamping force (180 pN) and TCEP concentration (2.5 mM). We cannot entirely exclude the possibility that under a different set of conditions multiple reaction mechanisms may appear. We also cannot conclusively exclude a narrow distribution of transition states until we build a much larger (10–100-fold larger) data set, but to our knowledge, this type of distribution has not yet been predicted by any theoretical or experimental findings.

Logarithmic Histogram Displays Two Reaction Mechanisms for TRX. In this study, the rates of disulfide reduction by TRX have been obtained by fitting a single and double exponential to the averaged ensemble of force-clamp traces, the bootstrapping method, and dwell time analysis. All of these methods point toward a double-exponential model describing the reduction kinetics. This double-exponential fit is most easily observed in the logarithmic histograms of the dwell times.

These results confirm and expand upon the conclusions reached by Wiita et al.¹⁸ in their recent study of force-dependent catalytic mechanisms of TRX, where forces in the range of 25–250 pN decreased TRX activity and forces from 250 to 600 pN increased the rate of disulfide reduction. These results were explained by a three-state kinetic model that predicted two separate transition states for the chemical reduction of disulfide bonds by TRX. The primary mode of catalysis requires binding the substrate to the enzyme and a reorientation of the substrate disulfide bond prior to nucleophilic attack by the catalytic cysteine of TRX. The secondary catalytic mechanism does not require this binding and reorientation. Its exact origin is not yet clear, but it appears to involve disulfide bond lengthening in the transition state of the chemical reaction.

In the studies by Wiita et al.,¹⁸ the rates of reduction at each force were obtained by fitting single exponentials to averaged force-clamp recordings. Thus, whereas the proposal for two kinetic pathways for TRX was developed from force-clamp data, this applied kinetic model could not be verified because it was not possible to resolve two reaction mechanisms at a given force simultaneously. Wiita et al. could only attempt to isolate the different reaction mechanisms by clamping $(I27_{SS})_8$ at either very high or low forces, where one mechanism predominates and the other is minimized. However, this method is imperfect because at every force there is always some contribution of the other reaction mechanism that is not accounted for in the single-exponential fit.

The current analytical methods, especially through the use of logarithmic histograms, can now resolve the two reaction mechanisms at a given force, an important improvement over previous methods of analysis. Such logarithmic histograms have another significant advantage in that they do not rely upon the potentially imprecise fitting of single exponentials to the averaged experimental data in order to obtain the mean reduction rate. Figure 6 and Table 2 also show that the use of logarithmic histograms identifies this ratio of amplitudes between the two reactions as 4.34 ± 0.41 . An earlier analysis of the three-state kinetic model predicted that the ratio of amplitudes between the primary and secondary reaction mechanisms should be ~ 4 at 100 pN.¹⁸ Although these two results are quite similar, the logarithmic histograms allow for the direct visualization of the ratio of amplitudes from the experimental data and do not rely on predictions of a complex kinetic model.

In Wiita et al.,¹⁸ the Bell model (eq 1) was used to relate the force-dependent kinetics of a given process to the physical distance required to reach the transition state (Δx). This Δx term can be used to resolve dynamic, sub-angstrom conformational changes that occur during enzymatic catalysis. However, to determine the value of Δx , the force-dependent kinetics of a given process must be measured as accurately as possible. Ideally, to obtain the most accurate force dependency of TRX reduction kinetics, logarithmic histograms of dwell times, such as that shown here at 100 pN, should be plotted over a wide range of forces. In this way, the rate of each mechanistic component and the relative amplitudes can be easily tracked and assessed as a function of force, offering the most insight into enzymatic conformational dynamics.

Conclusions and Perspectives

This article has provided an analysis of disulfide bond reduction kinetics at the single-molecule level. An extensive pool of data comprising thousands of single reduction events is recorded by force-clamp spectroscopy and analyzed using two separate approaches: (i) ensemble averaging of force-clamp recordings

(45) Bell, G. I. *Science* **1978**, *200*, 618–627.

with standard errors obtained by bootstrapping and (ii) dwell time analysis using linear and logarithmic histograms. The logarithmic histograms of dwell times with a square root ordinate of the number of events directly display the underlying rate constants, providing a useful tool for further force-clamp analysis.

In the case of TCEP, the kinetics of disulfide reduction can be explained in terms of a single reaction mechanism. However, there is still some possibility that a distribution of energetically similar transition states could be revealed by obtaining a much larger data set. Additionally, we cannot entirely exclude the possibility that under a different set of reagent concentration and clamping forces multiple reaction mechanisms may appear. In the case of TRX, we are indeed able to resolve two different kinetic processes. This result is supported by our earlier experiments with a number of different forces, where we proposed that there are two different mechanisms for TRX catalysis. Those earlier results could be expanded upon and refined through using logarithmic histograms of dwell times over a range of forces.

TCEP is a synthesized chemical reagent that is not present in biology, whereas thioredoxin is conserved throughout all living organisms. The presence of two well-defined reduction rates in the case of thioredoxin might have biological significance because thioredoxin regulates the redox state in organisms and the response of thioredoxin could depend on conditions of mechanical stress.

The study of TCEP and TRX could be refined through the collection of ever-larger data sets. At current levels of data throughput, a single operator requires 4–8 weeks of experiments

to obtain the number of events necessary to compile an accurate logarithmic histogram of dwell times. Thus, at the moment it may be impractical to obtain single data sets of > 10 000 events or smaller data sets at a series of forces. However, future improvements in our methods could significantly improve the rate of data collection, enhancing the utility of logarithmic histograms in analyzing force-clamp data.

It is clear that the various analyses presented here and, in particular, the logarithmic histograms of the dwell times can provide information from force-clamp spectroscopy data that could not be observed with previous methods.

Acknowledgment. We gratefully acknowledge discussions with members of the Fernandez laboratory. We thank Carmen Badilla for protein purification, Rodolfo Hermans for software programming, and Lorna Dougan for a careful reading of the manuscript. Our work was supported by the National Institutes of Health grants HL 66030 and HL 61228 to J.M.F, grant BIO2006-07332 from the Spanish Ministry of Education and Science to J.M.S.-R., and FEDER funds to J.M.S.-R.

Supporting Information Available: Data characterization procedure and information about the programs used here written with Igor Pro software (Wavematrix). This material is available free of charge via the Internet at <http://pubs.acs.org>.

LA702368B